



# Prospects of detecting dark matter through cosmic-ray antihelium with the antiproton constraints

Nan Li

*Institute of Theoretical Physics, Chinese Academy of Sciences*

Based on arXiv: 1808.03612v2

Mar 28, 2019

Antideuteron 2019, Los Angeles

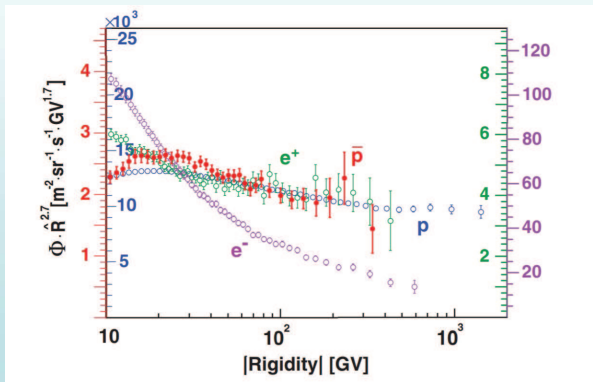


## Outline:

- The coalescence model
- The propagation of anti-nuclei in cosmic rays
- The upper limit of dark matter annihilation cross sections from the AMS-02  $\bar{p}/p$  data
- The detecting prospects of anti-Helium on AMS-02
- Conclusions

# Introduction

The existence of Dark Matter (DM) are supported by various observations, but the particle nature of DM is still largely unknown. High precision measurements of Cosmic Rays (CR) may shed light on the properties of DM.



AMS Coll., PRL 117 (2016) 091103

# Anti-nuclei in cosmic rays

Anti-nuclei in CR are important probes in Dark Matter indirect detection.

- The high production threshold boosts the secondary productions to high kinetic energies, leaving a high signal to background ratio in low energy regions.
- The production of anti-nuclei are highly correlated with anti-protons, the uncertainties of CR anti-nuclei can be well constrained by the CR anti-proton observations.

## coalescence model

Nucleons combine into a nucleus if the relative four-momenta of proper sets of nucleons is less than the coalescence momentum  $p_0$ .

# The coalescence criterion

## Coalescence criterion for $\overline{D}$

$$||k_{\overline{p}} - k_{\overline{n}}|| = \sqrt{(\Delta\vec{k})^2 - (\Delta E)^2} < p_0^{\overline{D}}.$$

## Coalescence criterion for ${}^3\overline{\text{He}}$

- Requiring the relative four-momenta of each pair of anti-nucleons smaller than  $p_0^{\overline{\text{He}}}$ . (*Nucleon Pair*)
- Using a circle with minimal radius to envelope the relative four-momenta of the anti-nucleons, and requiring the diameter of this circle less than  $p_0^{\overline{\text{He}}}$ . (*Minimal Circle*)
- Boosting the set of anti-nucleons into their center-of-mass frame, and requiring the momentum of each anti-nucleon smaller than  $p_0^{\overline{\text{He}}}/2$ . (*Afterburner*)

# The coalescence momentum

The coalescence momentum of  ${}^3\overline{\text{He}}$ :

Using the relation between  $p_0^{\overline{\text{He}}}$  and  $p_0^{\overline{\text{D}}}$ :

*E. Carlson et al., PRD 89 (2014) 076005*

- The binding energy relation:

$$p_0^{\overline{\text{He}}} = \sqrt{E_b^{3\overline{\text{He}}} / E_b^{\overline{\text{D}}}} p_0^{\overline{\text{D}}}$$

- Assuming  $p_0^{\overline{\text{He}}} / p_0^{\overline{\text{D}}} = p_0^{\text{He}} / p_0^{\text{D}}$ :

$$p_0^{\overline{\text{He}}} = \langle p_0^{\text{He}} / p_0^{\text{D}} \rangle p_0^{\overline{\text{D}}}$$

The ALICE group released the only  ${}^3\overline{\text{He}}$  data in  $pp$  collisions:

3 data points for  ${}^3\overline{\text{He}}$  in different  $p_T$  ranges and one data points for  $\overline{\text{T}}$ , at  $\sqrt{s} = 7$  TeV.

*ALICE Coll., PRC 97 (2018) 024615*

# Fitting the ALICE data

## Coalescence parameter $B_3$

$$E_{\overline{\text{He}}} \frac{d^3 N_{\overline{\text{He}}}}{d\vec{p}_{\overline{\text{He}}}^3} = B_3 \left( E_{\overline{p}} \frac{d^3 N_{\overline{p}}}{d\vec{p}_{\overline{p}}^3} \right)^2 \left( E_{\overline{n}} \frac{d^3 N_{\overline{n}}}{d\vec{p}_{\overline{n}}^3} \right), \quad \vec{p}_{\overline{p}} = \vec{p}_{\overline{n}} = \vec{p}_{\overline{\text{He}}}/3.$$

Convert  $B_3$  to coalescence momentum:

- Uncorrelated and isotropic momentum distributions:

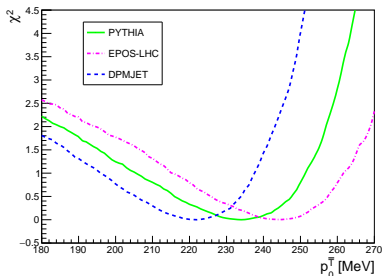
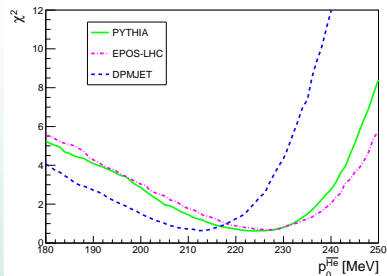
$$B_3 = \frac{m_{\text{He}}}{m_p^2 m_n} \left( \frac{\pi}{6} (p_0^{\overline{\text{He}}})^3 \right)^2$$

- Monte Carlo (MC) simulations:

Calculate the spectrum of  $\overline{\text{He}}$  for a series of  $p_0^{\overline{\text{He}}}$ , and make a  $\chi^2$  fitting to pick out the best-fit value.

MC generators: **PYTHIA, EPOS-LHC, DPMJET**

# Fitting the ALICE data

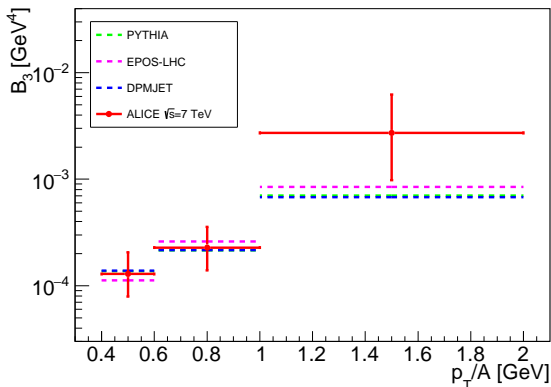


$$\chi_{\min}^2/d.o.f \sim 0.6/2$$

| MC generators:          | PYTHIA                             | EPOS-LHC                           | DPMJET            |
|-------------------------|------------------------------------|------------------------------------|-------------------|
| $p_0^{\text{He}}$ [MeV] | $224_{-16}^{+12}$ ( $254 \pm 14$ ) | $227_{-16}^{+11}$ ( $254 \pm 14$ ) | $212_{-13}^{+10}$ |
| $p_0^{\text{T}}$ [MeV]  | $234_{-29}^{+17}$ ( $266 \pm 22$ ) | $245_{-30}^{+17}$ ( $268 \pm 22$ ) | $222_{-26}^{+16}$ |



# Fitting the ALICE data

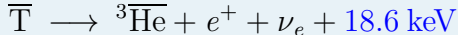


The  $p_T$  dependence are reproduced.

# The formation of ${}^3\overline{\text{He}}$

## Two possible channels to form a ${}^3\overline{\text{He}}$

- Direct formation ( $\overline{p}\overline{p}\overline{n}$ ):  
expected to be suppressed by Coulombian repulsion between the two antiprotons.
- The  $\beta$ -decay of anti-Triton ( $\overline{p}\overline{n}\overline{n}$ ):



The Coulombian repulsion may not be significant:

- $p_0^{\overline{\text{He}}}$  is only 4%  $\sim$  8% smaller than  $p_0^{\overline{\text{T}}}$
- Gamow factor:  $\mathcal{G} \sim \exp(-2\pi\alpha\frac{m_p}{p_0^{\overline{\text{He}}}}) \sim 0.8$

Both channels are included in our work.

# ${}^3\overline{\text{He}}$ from DM annihilation

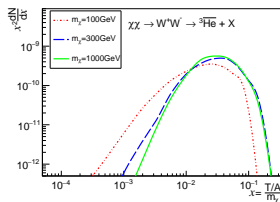
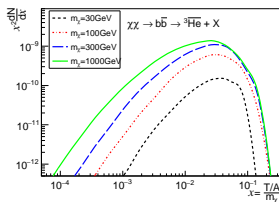
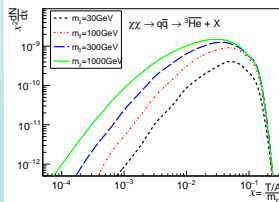
**PYTHIA** is used to simulate the hadronization after the DM annihilation.

$\chi\chi \rightarrow \text{Generic Resonance} \rightarrow q\bar{q} \text{ or } b\bar{b} \text{ or } W^+W^-$   
with  $m_\chi = 30, 100, 300, 1000 \text{ GeV}$ .

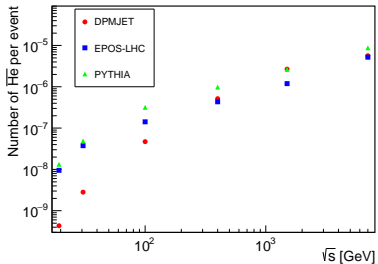
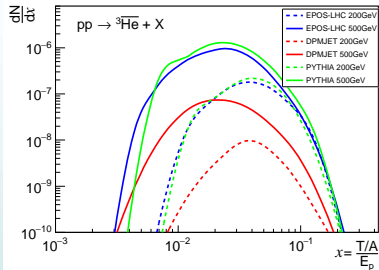
$\mathcal{O}(10^{11})$  collision events,  $\mathcal{O}(10^4)$   ${}^3\overline{\text{He}}$  produced for each case

The rescaled energy spectra of DM sourced  ${}^3\overline{\text{He}}$ :

$$p_0^{\overline{\text{He}}} = 224 \text{ MeV}, p_0^{\overline{\text{T}}} = 234 \text{ MeV}$$



# ${}^3\overline{\text{He}}$ from $pp$ -collisions



Left) The energy spectra of  ${}^3\overline{\text{He}}$  from  $pp$ -collisions, with the incident proton energy  $E = 200$  and  $500$  GeV, from **PYTHIA**, **EPOS-LHC** and **DPMJET**. Right) The total number of  ${}^3\overline{\text{He}}$  produced in  $pp$ -collisions at different  $\sqrt{s}$ , from the three MC generators.

The uncertainty from MC generators:  $\mathcal{O}(10)$

# The propagation of anti-nuclei in CR

## The diffusion equation

$$\frac{\partial \psi}{\partial t} = q(\vec{r}, p) + \vec{\nabla} \cdot (D_{xx} \vec{\nabla} \psi - \vec{V}_c \psi) + \frac{\partial}{\partial p} p^2 D_{pp} \frac{\partial}{\partial p} \frac{1}{p^2} \psi - \frac{\partial}{\partial p} \left[ \dot{p} \psi - \frac{p}{3} (\vec{\nabla} \cdot \vec{V}_c) \psi \right] - \frac{1}{\tau_f} \psi - \frac{1}{\tau_r} \psi$$

The equation is solved by the **GALPROP** v54 code.

Three propagation models:

A global Bayesian fitting to the AMS-02  $B/C$  ratio and proton flux

| Model | $r_h$ (kpc) | $z_h$ (kpc) | $D_0$ | $R_0$ (GV) | $\delta_1/\delta_2$ | $V_a$ (km/s) | $R_{ps}$ (GV) | $\gamma_{p1}/\gamma_{p2}$ |
|-------|-------------|-------------|-------|------------|---------------------|--------------|---------------|---------------------------|
| MIN   | 20          | 1.8         | 3.53  | 4.0        | 0.3/0.3             | 42.7         | 10.0          | 1.75/2.44                 |
| MED   | 20          | 3.2         | 6.50  | 4.0        | 0.29/0.29           | 44.8         | 10.0          | 1.79/2.45                 |
| MAX   | 20          | 6.0         | 10.6  | 4.0        | 0.29/0.29           | 43.4         | 10.0          | 1.81/2.46                 |

*H.-B. Jin et al., JCAP 09 (2015) 049*

# The source terms

The source term of DM  $\bar{A}$  ( $\bar{A} = \bar{p}, {}^3\bar{\text{He}}$ )

$$q_{\text{He}}(\vec{r}, p) = \frac{\rho_{\text{DM}}^2(\vec{r})}{2m_\chi^2} \langle \sigma v \rangle \frac{dN_{\bar{A}}}{dp}$$

Four DM profiles: Einasto, Isothermal, Moore, NFW

The source term of the secondary (tertiary)  $\bar{A}$

$$q(\vec{r}, p) = \sum_{i=p, \text{He}(\bar{p})} \sum_{j=\text{H}, \text{He}} n_j(\vec{r}) \int \beta_i c \sigma_{ij}^{\text{inel}}(p') \frac{dN_{\bar{A}}(p, p')}{dp} n_i(\vec{r}, p') dp'$$

The inelastic cross section  $\sigma_{ij}^{\text{inel}}$  are derived from MC generators.  
Only  $pp$  contributions are included for  ${}^3\bar{\text{He}}$ .

# The interaction cross sections

The inelastic interaction rate  $\Gamma_{\text{int}} = 1/\tau_f$ ,  
scattering rate between  $\bar{A}$  and the interstellar gas:

$$\Gamma_{\text{int}} = (n_{\text{H}} + 4^{2/3} n_{\text{He}}) v \sigma_{\bar{A}p}$$

$n_{\text{He}}/n_{\text{H}} = 0.11$  (GALPROP default)

$\sigma_{\overline{\text{He}p}}$  data are not available,  $\sigma_{\overline{\text{He}p}} = \sigma_{\text{He}\bar{p}}$  assumed by CP-invariance

## A parametrization of $\sigma_{A\bar{p}}$

$$\sigma_{A\bar{p}} = A^{2/3} \left[ 48.2 + 19 x^{-0.55} + (0.1 - 0.18 x^{-1.2})Z + 0.0012 x^{-1.5} Z^2 \right] \text{mb}$$

where  $x = T/(A \cdot \text{GeV})$ . For  $\sigma_{\overline{\text{He}p}}$ ,  $A = 3$ ,  $Z = 2$ .

# The solar modulation

The spectra of CR particles are effected by the solar wind and the magnetic field of solar system.

## Force Field Approximation

$$\Phi_{A,Z}^{TOA}(T_{TOA}) = \left( \frac{2m_A A T_{TOA} + A^2 T_{TOA}^2}{2m_A A T_{IS} + A^2 T_{IS}^2} \right) \Phi_{A,Z}^{IS}(T_{IS})$$

where  $T_{IS} = T_{TOA} + (e\phi_F|Z|/A)$ .

The Fisk potential  $\phi_F = 550$  MV.



# Upper limit of DM annihilation cross section

AMS-02 published the so far most accurate antiproton flux, and this measurement would give a stringent limitation on the DM annihilation cross section.

We use the frequentist  $\chi^2$ -analyse to derive the 95% CL upper limits on the DM annihilation cross section from the AMS-02  $\bar{p}/p$  data.

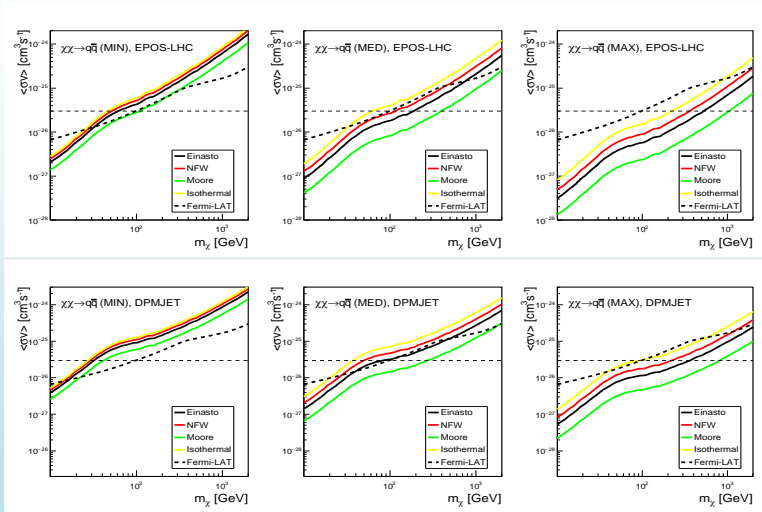
First calculate the minimal value  $\chi_{min}$ , 95% CL corresponding to  $\Delta\chi^2 = 3.84$  for one parameter.

**NA49** data:

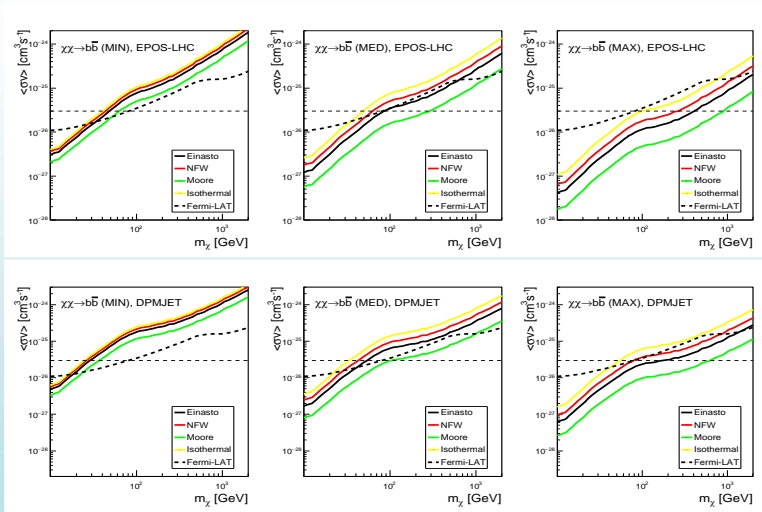
*NA49 Coll., Eur.Phys.J.C65:9-63 (2010)*

**PYTHIA** overestimate the production of  $\bar{p}$  from  $pp$  collisions at low  $\sqrt{s}$ , **EPOS-LHC** and **DPMJET** consist with the NA49 data.

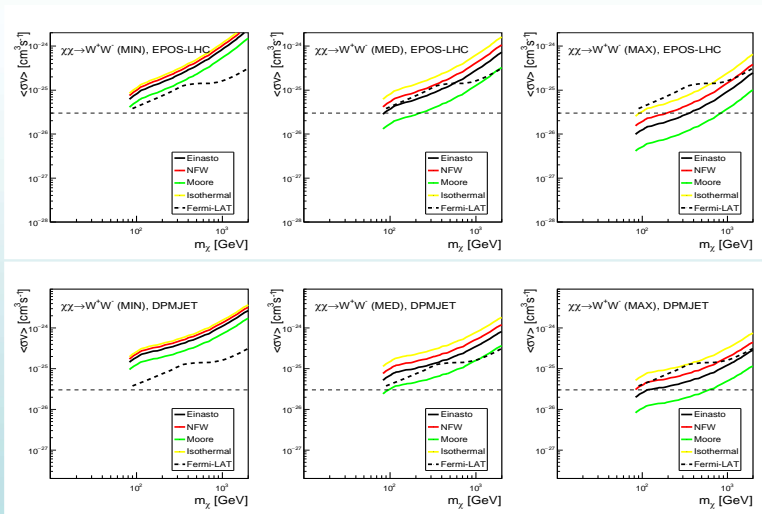
# The upper limit of DM cross sections ( $q\bar{q}$ )



# The upper limit of DM cross sections ( $b\bar{b}$ )



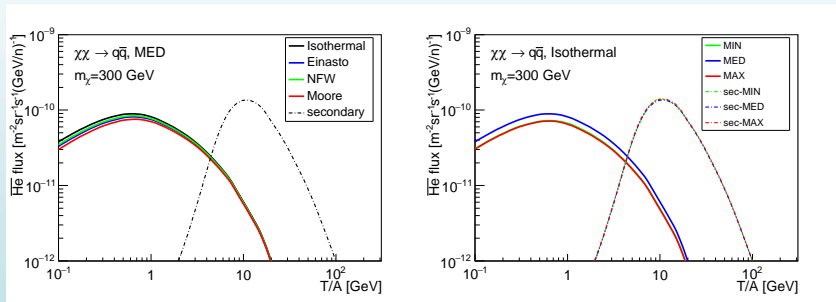
# The upper limit of DM cross sections ( $W^+W^-$ )



# The flux of ${}^3\overline{\text{He}}$

An advantage of constraining  ${}^3\overline{\text{He}}$  with  $\bar{p}$ : greatly reducing the uncertainties.

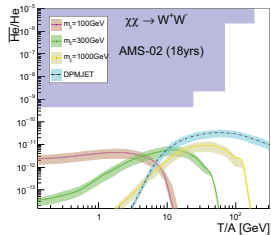
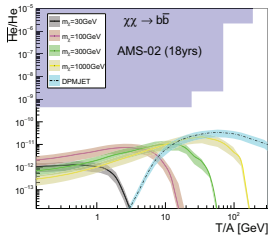
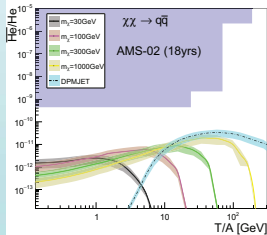
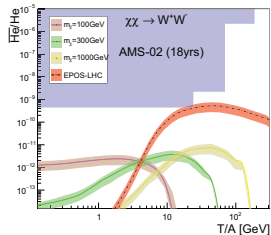
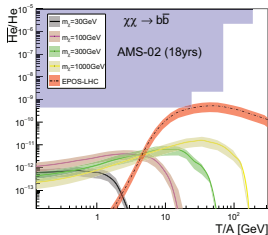
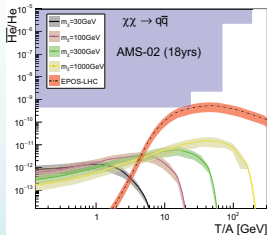
Fixed  $\langle \sigma v \rangle$ : propagation models  $\mathcal{O}(10)$     DM profiles  $\mathcal{O}(10)$   
 $\bar{p}$  constrained  $\langle \sigma v \rangle$ : propagation models 30%    DM profiles 30%



*Left*) Differences between the DM profiles. *Right*) Differences between the propagation models.

# The detecting prospects on AMS-02

Propagation model: MED      DM profile: Isothermal



# The prospective ${}^3\overline{\text{He}}$ number on AMS-02

The number of  ${}^3\overline{\text{He}}$  observed on AMS-02:

$$N = \int_{T_{\min}}^{T_{\max}} \eta \Phi_{\overline{\text{He}}} \mathcal{A} t dT$$

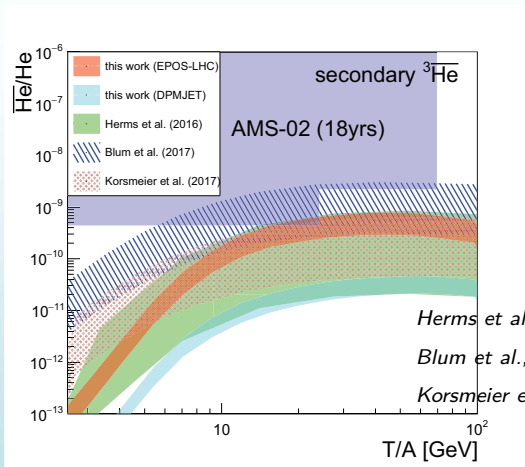
Most optimistic assumption:

$$\eta = 1, \mathcal{A} = 0.5 \text{m}^2 \text{sr (geometric acceptance),}$$

$$t = 18 \text{ years, } T_{\min(\max)}/A = 0.1 \text{ GeV (1 TeV).}$$

| $m_\chi$ (GeV) | $\chi\chi \rightarrow q\bar{q}$ | $\chi\chi \rightarrow b\bar{b}$  | $\chi\chi \rightarrow W^+W^-$  |  |
|----------------|---------------------------------|--|--|--|
| DM             | 30                              | $0.084^{+0.038}_{-0.040}$ (0.153 <sup>+0.070</sup> <sub>-0.073</sub> ) | $0.041^{+0.020}_{-0.018}$ (0.073 <sup>+0.036</sup> <sub>-0.032</sub> ) | —  |
|                | 100                             | $0.153^{+0.065}_{-0.072}$ (0.269 <sup>+0.114</sup> <sub>-0.127</sub> ) | $0.227^{+0.107}_{-0.103}$ (0.419 <sup>+0.198</sup> <sub>-0.190</sub> ) | $0.164^{+0.077}_{-0.076}$ (0.304 <sup>+0.143</sup> <sub>-0.141</sub> ) |
|                | 300                             | $0.122^{+0.055}_{-0.056}$ (0.179 <sup>+0.081</sup> <sub>-0.082</sub> ) | $0.160^{+0.074}_{-0.074}$ (0.256 <sup>+0.118</sup> <sub>-0.118</sub> ) | $0.054^{+0.025}_{-0.025}$ (0.084 <sup>+0.039</sup> <sub>-0.039</sub> ) |
|                | 1000                            | $0.106^{+0.048}_{-0.048}$ (0.138 <sup>+0.063</sup> <sub>-0.063</sub> ) | $0.131^{+0.058}_{-0.061}$ (0.179 <sup>+0.079</sup> <sub>-0.083</sub> ) | $0.015^{+0.007}_{-0.007}$ (0.019 <sup>+0.009</sup> <sub>-0.009</sub> ) |
| Secondary      |                                 | $0.986^{+0.437}_{-0.455}$  | $(0.054^{+0.021}_{-0.021})$  |  |

# A comparison of secondary $\overline{^3\text{He}}$



*Herms et al., JCAP 1702 (2017) 018*

*Blum et al., PRD 96 (2017) 103021*

*Korsmeier et al., PRD 97 (2018) 103011*

Fluxes overlap at  $T/A > 10$  GeV !

A candidate event of  $\overline{^3\text{He}}$  with momentum  $40.3 \pm 2.9$  GeV

*S. Ting, <https://indico.cern.ch/event/592392>*



# Conclusions

- AMS-02 is likely to detect the secondary  ${}^3\overline{\text{He}}$
- AMS-02 is unlikely to detect the  ${}^3\overline{\text{He}}$  from DM
- The sensitivity of next generation of detectors should improve about two order of magnitude to detect the  ${}^3\overline{\text{He}}$  from DM



Thank You!